C. R. Physique 11 (2010) 236–244

Contents lists available at ScienceDirect

Comptes Rendus Physique

www.sciencedirect.com

Computational metallurgy and changes of scale / Métallurgie numérique et changements d'échelle

Mesoscopic modelling of precipitation: A tool for extracting physical parameters of phase transformations in metallic alloys

Modélisation mésoscopique de la précipitation : Un outil pour extraire les paramètres physiques des transformations de phase dans des alliages métalliques

Alexis Deschamps [a,*], Michel Perez [b]

[a] SIMAP, Grenoble INP, UMR CNRS 5266, Université Joseph-Fourier, 1130, rue de la Piscine, BP 75, 38402 St Martin d'Hérès cedex, France
[b] Université de Lyon, INSA Lyon, MATEIS, UMR CNRS 5510, 7, avenue Jean-Capelle, 69621 Villeurbanne cedex, France

ARTICLE INFO

Article history:
Available online 23 August 2010

Keywords:
Precipitation
Classical Nucleation and Growth theories
Class model

Mots-clés :
Précipitation
Théorie Classique de la Germination/Croissance
Modèle par classes de taille

ABSTRACT

Classical Nucleation and Growth Theories provide a compelling framework predicting the nucleation and growth of precipitates. When implemented in a class model, such an approach provides the time evolution of the Particle Size Distribution. It is shown in this article that a reversion treatment (instantaneous heating of the microstructure to a temperature high enough to induce some dissolution of the precipitates) can be used to calibrate all physical parameters of the model independently: (i) the solubility limit of alloying element is related to the equilibrium volume fraction; (ii) the interfacial energy is related to the minimum of volume fraction evolution; and (iii) the diffusion constant is related to the kinetics of the precipitate radii evolution.

RÉSUMÉ

La Théorie Classique de la Germination/Croissance est un puissant outil pour prédire des cinétiques de précipitation. Implémentée dans un modèle par classes de taille, cette approche permet de prédire l'évolution de la distribution de taille des précipités. Dans cet article, il est montré qu'un traitement de réversion (chauffage à une température qui entraine une dissolution partielle des précipités) peut être utilisé pour déterminer de façon indépendante tous les paramètres physiques du modèle: (i) la limite de solubilité est liée à la fraction volumique précipitée d'équilibre, (ii) l'énergie d'interface est liée au minimum de la fraction volumique précipitée, et (iii) le coefficient de diffusion est lié à la cinétique d'évolution du rayon moyen des précipités.

1. Introduction

Fine scale precipitation is one of the most important features of the microstructure of metallic alloys for the control of many of their properties [1]. Nanoscale precipitates have a direct impact on the mechanical properties, particularly on strength [2], and many indirect impacts such as their influence on recrystallization [3] and/or grain growth [4,5]. The op-

* Corresponding author.
E-mail addresses: alexis.deschamps@grenoble-inp.fr (A. Deschamps), michel.perez@insa-lyon.fr (M. Perez).

1631-0705/$ – see front matter
doi:10.1016/j.crhy.2010.07.005

timization of the end properties requires controlling the formation of the precipitates, particularly in terms of size and dispersion (volume fraction and number density). A given microstructure is obtained by following a sequence of heat treatments, going through different stages that are generally artificially separated into nucleation (appearance) of new particles, growth (increase of particle size at constant number per unit volume), and coarsening (diminution of the number of particles at constant volume fraction). Practically, these stages are, of course, inter-related, and a complete description of precipitation requires also considering other processes such as shrinkage (reverse of growth), heterogeneous nucleation and competition between different forming phases that can be stable or metastable.

The scientific field of precipitation modelling has been extremely active in the last decade. Modelling the processes of precipitation can be achieved at different scales, with corresponding tools, with each having its own advantages and disadvantages:

(i) At the atomic scale, Atomic Kinetic Monte Carlo methods are widely used [6]. With the currently available computer resources, these methods make it possible to simulate both the initial and relatively late stages of the precipitation process, including coarsening. Based on proper ab initio modelling, they provide a very sound description of the kinetic path, and are well adapted to tackle difficult problems such as precipitation in concentrated materials. However they are strongly restricted in terms of modelling of real systems, namely in their capacity to describe multi-component systems (more than ternary becomes difficult), phases of complicated crystallography, heterogeneous precipitation and elastic effects.

(ii) At the mesoscopic level, several modelling approaches exist, based on a continuous or semi-continuous description of matter. The two most common techniques are the cluster dynamics method, based on the thermodynamics of condensation/evaporation kinetics of atoms on precipitates [7], and the class modelling method, based on the application of the classical nucleation and growth equations to a discrete precipitate size distribution [8–14]. Although these methods offer a less precise description of the precipitation processes, they are well adapted to tackle complicated problems such as multi-component, multi-phase precipitation or non-isothermal precipitation.

(iii) At the macroscopic scale, one finds semi-phenomenological approaches such as the Johnson–Mehl–Avrami–Kolmogorov (JMAK) models [15,16]. These models generally describe only the fraction transformed and not the scale of the microstructures.

One common difficulty in applying models to describe a precipitation process is to obtain reliable data for the physical parameters of the phase transformation. One can list the main parameters in a simple binary alloy, for which the solid solution obeys a simple thermodynamics (e.g. diluted regular solution) as: (i) the equilibrium solubility of the solute; (ii) the diffusion constant of the solute in the matrix; and (iii) the interfacial energy between precipitate and matrix. Moreover, if nucleation of the precipitates is not perfectly homogeneous (which is a common complication), one additional parameter appears, related to the heterogeneous character of nucleation. Since these parameters are not generally known with sufficient precision in the literature, they must be obtained by adjusting the models to experimental data. This is a slightly hazardous task, because obtaining large sets of quantitative data is not an easy task, and the effects of the different parameters on a given feature of the microstructure are generally inter-related. One example is the precipitate coarsening rate predicted by the LSW law, which depends on three parameters (solute solubility, diffusion coefficient, and interfacial energy) [8].

The present article will present a type of precipitation model that has seen a strong development in the last years, which is the class model, based on Classical Nucleation and Growth Theories (CNGTs) [8–14]. In this model, the precipitates are distributed in classes of size. The evolution of precipitates in each class is computed using classical equations for growth and dissolution, and assuming simple equilibrium conditions at the interfaces (local thermodynamic equilibrium). The explicit consideration of the precipitate size distributions has proven to be very powerful to describe complicated effects arising from non-isothermal precipitation kinetics, and therefore these models have been shown to be applicable to wide ranges of complicated situations. We will show in the present article that these models can be used with a methodology by which all parameters of a precipitation model can be obtained independently from a comparison with experimental data along non-isothermal heat treatments. In Section 2 the class model will be presented; in Section 3 the methodology for obtaining the different parameters will be detailed, and the influence of a number of parameters will be investigated.

2. Class model for precipitation

The class model for precipitation aims at describing the quantitative time evolution of the precipitation state, namely the particle size distribution, the volume fraction and the number density of precipitates. The precipitate size distribution is discretized into several size classes. The time evolution of the radius of each class is calculated as a function of temperature, solute content, solubility limit and diffusivity. Nucleation can eventually take place, thus adding new classes of precipitates.

For the sake of simplicity, in this article, we will restrict the use of the class model to cases where: (i) no nucleation occur; (ii) precipitates are spherical; (iii) the alloy is binary; and (iv) all precipitate classes are composed of the matrix element and the alloying element (fraction X^p). For more complex cases see Ref. [13].

2.1. Description of the Particle Size Distribution (PSD)

The continuous size distribution is discretized into a large number of size classes. A size class is defined by: (i) its radius R_i; (ii) its number of precipitates N_i per unit volume; and (iii) its chemistry X^p (fraction of alloying element within precipitate). The total number of precipitates N per unit volume is then given by

$$N = \sum_i N_i \tag{1}$$

and the mean radius $\bar{R}$ of the distribution is

$$\bar{R} = \frac{1}{N} \sum_i R_i N_i \tag{2}$$

The precipitate volume fraction f_T is then given by

$$f_T = \frac{4}{3}\pi \sum_i N_i R_i^3 \tag{3}$$

Finally, the mass balance sets the amount of solute atoms X remaining in solid solution from the knowledge of the particle size distribution and the total amount of alloying element X^0:

$$X = \frac{X^0 - \alpha f_T X^p}{1 - \alpha f_T} \tag{4}$$

where $\alpha = v_{at}^M / v_{at}^p$ is the ratio of matrix to precipitates atomic volumes (mean volume per atom).

2.2. Evolution equations

In binary alloys, the diffusion controlled growth rate of spherical precipitates (molar composition X^p, radius R_i) embedded in a supersaturated solid solution (mean solute mole fraction in the matrix X, equilibrium solute mole fraction X^e at the precipitate/matrix interface) has been provided by Zener [17] under the assumption of small supersaturation ($X^0 - X^e \ll \alpha X^p - X^e$):

$$\frac{\mathrm{d}R_i}{\mathrm{d}t} = \frac{D}{R_i} \frac{X - X^e}{\alpha X^p - X^e} \tag{5}$$

Interface curvature plays an important role on equilibrium mole fraction X^e; this is the so-called Gibbs–Thomson effect [18–21]. Hence, in a stoichiometric binary precipitate of composition X^p, radius R_i and matrix/precipitate surface energy γ, the precipitate/matrix interface equilibrium mole fractions are modified [22]:

$$X^e(R_i) = X^e \exp\left(\frac{2\gamma v_{at}^p}{X_i^p R_i k_B T} \right) \tag{6}$$

where k_B is Boltzman's constant and T is the absolute temperature. This leads to the following set of growth equations for each class i:

$$\frac{\mathrm{d}R_i}{\mathrm{d}t} = \frac{D}{R_i} \frac{X - X^e(R_i)}{\alpha X^p - X^e(R_i)} \tag{7}$$

Note that Eq. (7) combined with Eq. (6) is perfectly adapted to describe the coarsening regime, where shrinking of small precipitates occurs to the benefit of large ones due to Gibbs–Thomson effects. The critical radius R^* is the radius which separates the growing precipitates ($R > R^*$ meaning $X^e < X$) and the ones that shrink ($R < R^*$ meaning $X_i > X$), i.e. $dR/dt(R^*) = 0$. Using Eq. (6) leads to:

$$R^* = \frac{R_0}{\ln(X/X^e)} \quad \text{with } R_0 = \frac{2\gamma v_{at}^p}{X^p k_B T} \tag{8}$$

2.3. Implementation

The time evolution of each size class radius is calculated, the size class population remaining constant. At each time step, the new radius of all existing classes is calculated according to:

$$R_i(t + \Delta t) = R_i(t) + \frac{\mathrm{d}R_i}{\mathrm{d}t} \times \Delta t \tag{9}$$

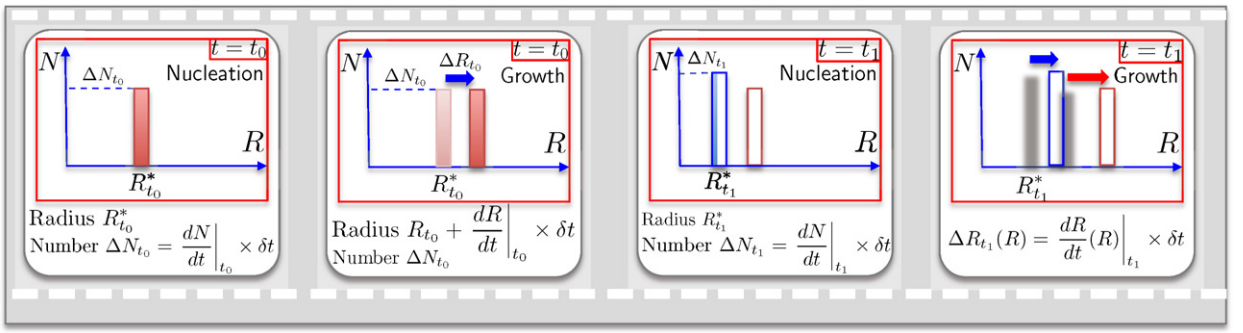

Fig. 1. Nucleation-growth sequence with a class model. At each time step, a new class is created and all existing classes grow according to classical nucleation and growth theories.

Fig. 1. Séquence de germination-croissance avec un modèle par classes. A chaque pas de temps, une nouvelle classe est créée et toutes les classes existantes croissent.

where the growth rate is given by Eq. (7). Fig. 1 details how growth and, if necessary, nucleation are managed within this approach.

An adaptive time step is also implemented in order to accelerate the simulation within reasonable accuracy: a too large time step may lead to numerical instabilities (oscillations) and/or aberrations (negative concentrations). A logarithmic increment of the time step is first performed ($\Delta t \to 1.1\Delta t$). The new time step Δt is accepted if: (i) the solute concentration ranges between 0 and 1; and (ii) the critical radius R^* (which is the most sensitive variable of the model) does not vary more than 1% between each time step. If either of these conditions is not fulfilled, the program returns to the previous time step and makes a new attempt with a smaller time step (typically $\Delta t \to \Delta t/2$). This last step can be repeated as many times as necessary.

In this approach, note that the number of classes decreases during the coarsening stage: classes smaller than the critical size ($R_i < R^*$) shrink, until they completely disappear.[1] To keep an accurate description of the PSD, a minimum number of classes should exist (typically 500). Therefore, if the distance (in terms of radius) between two adjacent classes is too large, a new class is artificially created between these two classes, its precipitate number density being adjusted to keep constant both the distribution density and the total precipitate volume fraction (more detail on class management can be found in Ref. [13]).

3. Methodology for an independent measurement of precipitate parameters

The idea behind this methodology is to separate the kinetic aspects from the thermodynamic aspects of precipitation. The thermodynamic properties determine the precipitate stability. This encompasses both the equilibrium stability (represented by the dependence of solute solubility on temperature) and the stability of precipitates of finite size (Gibbs–Thomson effect, whose magnitude depends on the interfacial energy). A convenient way to estimate experimentally the precipitate stability is to rapidly heat up a sample containing small scale precipitates. At a given temperature, the precipitates become unstable, and start to dissolve. The magnitude of this dissolution depends critically on the Gibbs–Thomson effect, and therefore both on the equilibrium solubility and on the interfacial energy. Let us study in some detail the sequence of events which happen during a so-called reversion experiment, which brings a sample containing precipitates rapidly to a higher temperature.

In the framework of mesoscopic precipitation modelling, an important parameter is the solute fraction at the precipitate/matrix interface. If this concentration is lower than the average matrix fraction, the precipitate grows, and if it is larger, the precipitates shrinks. This can be translated in the definition of a critical radius R^* (see Eq. (8)).

For a given solute concentration, R^* increases with temperature, meaning that precipitates of a given size R will become unstable when the temperature becomes sufficient high that $R^* > R$. On the other hand, for a given temperature, if the solute concentration increases (which happens when some precipitates dissolve), R^* is observed to decrease, so that precipitates that were unstable at a given time can regain stability once the solute content has reached a value, which is sufficiently high. Thus, the evolution of a precipitate of a given size during a non-isothermal heat treatment is a complicated interplay between the evolution of the precipitate radius (resulting from growth or dissolution) and of the critical radius (resulting from changes in temperature or solute content).

As a model system we will consider the Fe–Cu system, with precipitation of pure Cu in Fe ($X^p = 1$). Precipitates in this system are spherical, the atomic volume inside the precipitates is similar to that in the matrix and the difference can be neglected in first approximation ($\alpha = 1$). For the thermodynamics of the system we will use the same equation for solubility as determined in [23]:

[1] A class is deleted from the distribution if its radius is lower than 0.1 nm.

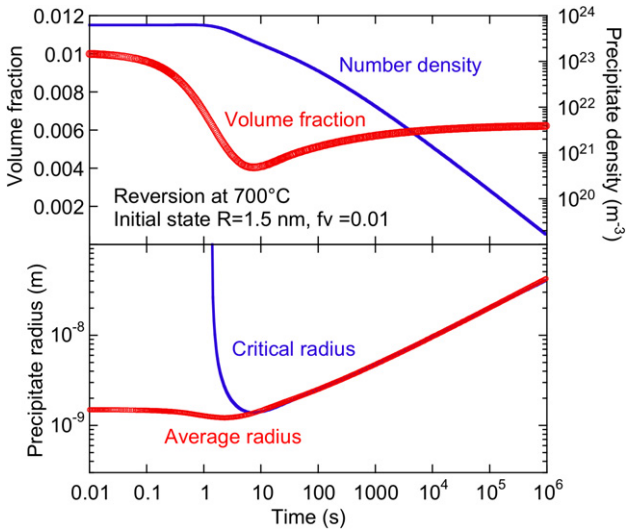

Fig. 2. A reversion treatment: after a first treatment resulting in a radius of 1.5 nm and a volume fraction of 1%, an isothermal treatment (reversion) at 700 °C is performed. The mean radius suddenly drops (shrinkage) and then starts to increase (coarsening). Interfacial energy is $\gamma = 0.25$ J/m^2.

Fig. 2. Traitement de réversion : un premier traitement de précipitation donne lieu à un rayon moyen de 1.5 nm et une fraction volumique précipitée de 1 %. Ensuite, un traitement isotherme (réversion) à 700 °C est effectué. Le rayon moyen diminue alors fortement (dissolution), puis croit de nouveau (mûrissement). L'énergie d'interface est $\gamma = 0{,}25$ J/m^2.

$$\log_{10} C^e\ [\text{wt\%}] = \frac{5\,771\,323}{T^2} - \frac{15\,763.84}{T} + 9.944961 \tag{10}$$

and

$$X^e = \frac{M_{\text{Fe}}}{M_{\text{Cu}}} \frac{C^e\ [\text{wt\%}]}{100} \tag{11}$$

We will consider a total solute concentration of 1.4 wt%, which corresponds to 1.23 at% ($X^0 = 0.0123$). We will assume an interfacial energy for the precipitates $\gamma = 0.25$ J/m^2, and the diffusion constant as:

$$D = D_0 \exp\left(\frac{Q}{RT}\right) \tag{12}$$

with $D_0 = 6 \times 10^{-8}$ m^2/s and $Q = 166\,400$ J/mol.

In order to describe a reversion experiment, it is not necessary to take into account any parameters for nucleation, since we will consider precipitates that are already present in the initial microstructure, the only thing that can happen to these particles is that they dissolve or they grow. Thus, the behavior of precipitates along such thermal paths will be influenced by all parameters except those for nucleation. Fig. 2 shows the reversion behavior on an initial precipitation state with an initial average radius of 1.5 nm and a phase fraction of 1%. The initial precipitate size distribution is taken as a log-normal distribution with a relative standard deviation of 0.2, which corresponds approximately to what is found in many experimental situations.

When such a microstructure is instantaneously heated to a temperature high enough to induce some dissolution of the precipitates, a three stage behaviour is observed:

(1) In a first stage, the volume fraction decreases rapidly, meaning that the destabilized precipitates start to dissolve. The average precipitate size actually does not change much at this stage, which could appear surprising at first thought. Actually the evaluation of the precipitate size distribution at different times during this stage provides an interpretation of this relatively constant average radius: whereas almost all precipitates shrink (decease of the mean radius), the smallest precipitates dissolve/disappear (increase of the mean radius). The net result is that the average value of the particle size stays rather constant.
(2) In a second stage, the volume fraction reaches a minimum. It is observed that this minimum coincides with the equality of the critical and average radii. In fact, at the constant temperature of the reversion experiment, when the unstable precipitates dissolve, the solute content of the matrix increases, resulting in a decrease of the critical radius, which gives additional stability to the precipitates that remain. At the point where the average and critical radii are equal, dissolution stops.
(3) In a third stage, the precipitate size increases rapidly, and the volume fraction increases more slowly towards an equilibrium value at the heat treatment temperature. During this stage, the critical radius remains at a size comparable to

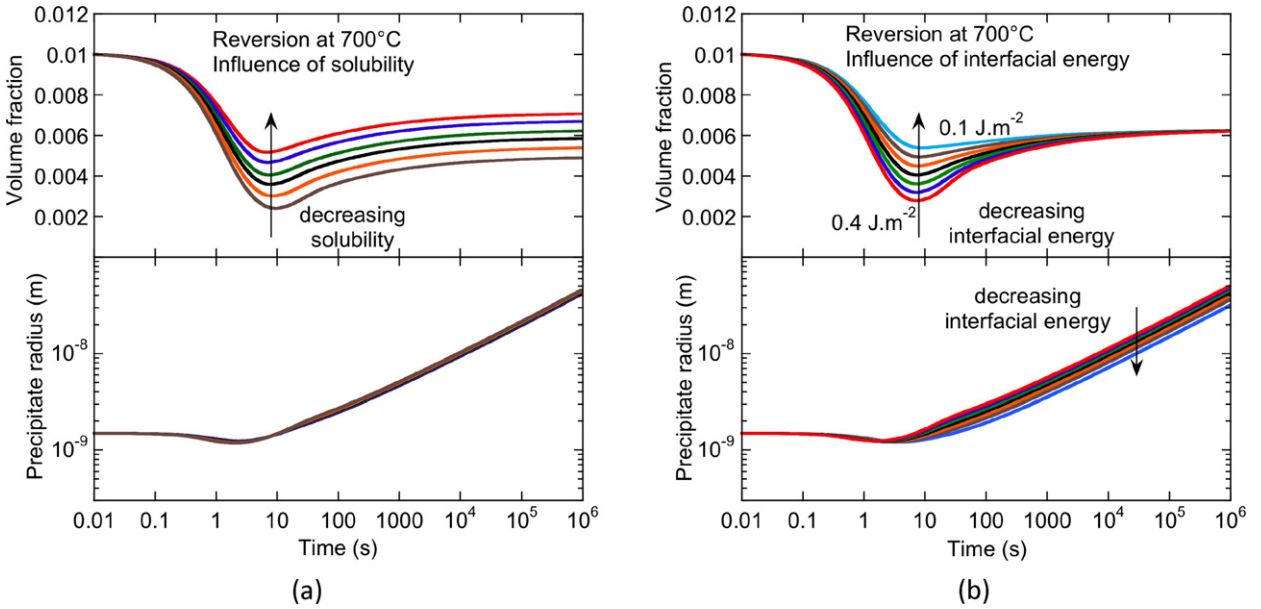

Fig. 3. Evolution of volume fraction and precipitate size for different values of (a) the equilibrium solubility at the reversion temperature (here 700 °C), and (b) the interfacial energy.

Fig. 3. Evolution de la fraction volumique précipitée pour différentes valeurs de (a) la limite de solubilité à 700 °C, et (b) l'énergie d'interface.

the average precipitate size. This stage is a coarsening stage. The fact that the precipitate volume fraction evolves is a result of the growing precipitate size: at each time step the volume fraction is at a value that ensures equilibrium with the average precipitate size R. The mass balance (Eq. (4)) leads to:

$$f_T = X^0 - X^e \exp\left(\frac{R_0}{R}\right) \tag{13}$$

Now it is possible to evaluate the effects of the three main parameters of precipitation (excluding nucleation, which does not intervene in reversion treatments) on the reversion process.

Fig. 3(a) shows the evolution of the volume fraction and precipitate size for different values of the equilibrium solubility at the reversion temperature (here 700 °C). Obviously, the value of solubility at the reversion temperature acts on the equilibrium volume fraction at the end of the heat treatment. This parameter also has a strong influence on the minimum volume fraction, through its influence on precipitate stability. Interestingly, the effect of the solubility on the evolution of the precipitate radius is however very small.

Fig. 3(b) shows the same evolution, when changing the interfacial energy. In this case, the equilibrium volume fraction is not changed, however, the minimum volume fraction is strongly affected. This behaviour is related to the influence of interfacial energy on the stability of precipitates of finite size (Gibbs–Thomson effect). The effect of interfacial energy on the evolution of precipitate size is now larger. Notably, the simulations confirm that the coarsening rate (albeit still with a time exponent of 1/3) is lower when the interfacial energy is lower. However, it appears very clearly that the sensitivity to the interfacial energy of the coarsening rate is much lower than that of the minimum volume fraction during the reversion experiment.

Fig. 4 shows the same evolution, when changing the diffusion constant. Clearly, the only influence of this parameter is to change the kinetics of the reversion process: changing the diffusion constant simply shifts the curves by a time constant.

From these results a methodology for the calibration of the physical parameters of a precipitating system can thus be devised:

(i) Calibrate the solubility on equilibrium volume fraction;
(ii) Calibrate the interfacial energy on the minimum of volume fraction;
(iii) Calibrate the diffusion constant on the kinetics of the precipitate evolution.

This methodology enables an independent calibration of these parameters, without any interference with nucleation, which can be studied separately during heat treatments performed from the solid solution. Existing data in the literature have already made use of this methodology to calibrate precipitate models both in aluminium alloys and in the Fe–Cu system.

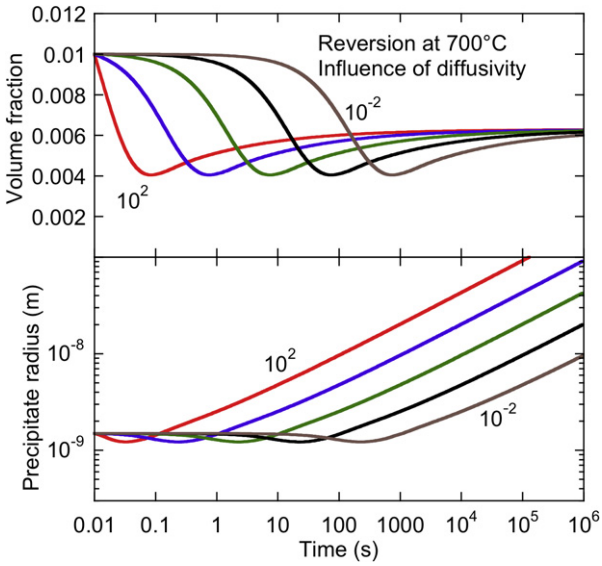

Fig. 4. Evolution of volume fraction and precipitate size for different values of the diffusion constant (from left to right: 10^2, 10^1, 10^0, 10^{-1} and 10^{-2}) relative to the initial value defined in the text.

Fig. 4. Évolution de la fraction volumique précipitée et du rayon moyen pour différentes valeurs du coefficient de diffusion (de gauche à droite : 10^2, 10^1, 10^0, 10^{-1} et 10^{-2}) en relatif par rapport à la valeur donnée dans le texte.

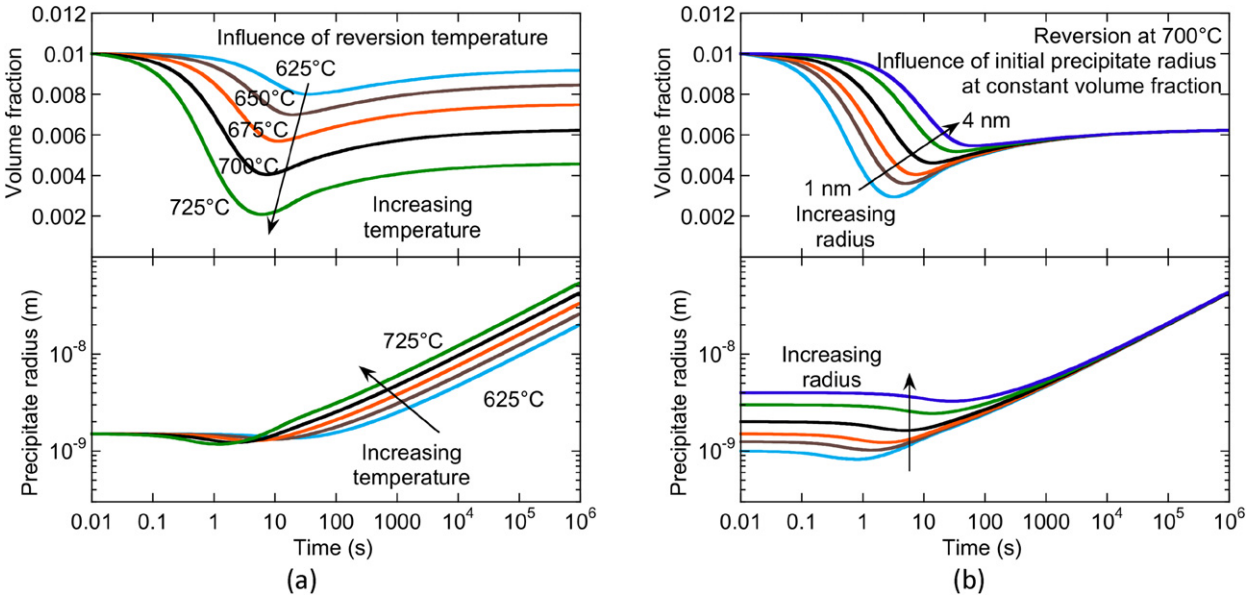

Fig. 5. Evolution of volume fraction and precipitate size for different values of (a) the reversion temperature, and (b) the initial average radius.

Fig. 5. Evolution de la fraction volumique précipitée pour différentes valeurs de (a) la température de réversion, et (b) la valeur initiale du rayon moyen de la distribution de taille des précipités.

Next, the effect of temperature on these physical parameters can be studied by performing reversion experiments with the same initial microstructure but at different temperatures. Fig. 5(a) shows the reversion behaviour as a function of the temperature of the experiment. The influence of temperature on precipitate volume fraction is similar to a solubility change, acting simultaneously on the minimum volume fraction and the equilibrium one. However, in this case the radius evolution is affected as well, especially in the coarsening regime.

Now it is interesting to evaluate how the reversion behaviour depends on the parameters of the initial precipitate microstructure, before the reversion experiment is performed. We will keep constant the type of precipitate size distribution (PSD) (namely a log normal distribution), and change independently its three parameters, namely the average radius, the width of the precipitate size distribution and the volume fraction.

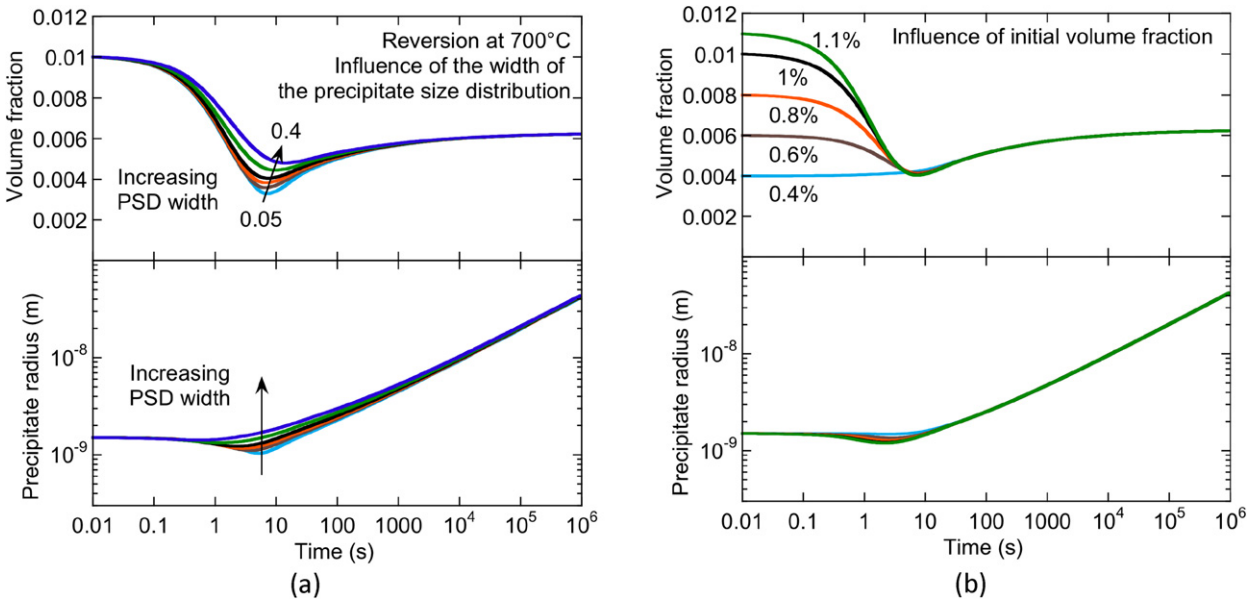

Fig. 6. Evolution of volume fraction and precipitate size for different values of (a) the precipitate size distribution width, and (b) the initial volume fraction.
Fig. 6. Evolution de la fraction volumique précipitée pour différentes valeurs de (a) la largeur de la distribution de taille des précipités, et (b) la valeur initiale de la fraction volumique précipitée.

Fig. 5(b) shows the effect of changing the value of the average radius. When precipitates are initially larger, they are more stable through the Gibbs–Thomson effect, and thus dissolve more slowly and to a smaller extent. After this initial stage, however, all microstructures converge to the same coarsening stage.

Fig. 6(a) shows the effect of changing the PSD width. This effect is observed to be very small as compared to the effect of the other parameters of the microstructure. When the PSD is wide, the extent of dissolution is smaller. This can be understood by the fact that the PSD in this case contains more large particles that will experience a smaller amount of dissolution, whereas the smaller precipitates, whatever the width of the distributions, experience dissolution in any case.

Finally, Fig. 6(b) shows the effect of changing the volume fraction. Changing the initial volume fraction (at constant precipitate radius) has very little influence on the precipitate size evolution. The volume fraction evolution also follows a common behaviour as soon as the minimum volume fraction is reached. This behaviour, which could appear surprising at first, comes from a compensation between the dissolution rate of precipitates and the solute content: when the initial volume fraction is larger, the solute content is smaller, thus the critical radius is larger and the precipitates are more unstable. As a consequence they dissolve faster and join the other particles that have dissolved less or not at all for the lowest initial volume fraction.

In conclusion, it should be mentioned that it is very difficult to design initial microstructures where one parameter is changed without changing the other ones.

4. Conclusion

Class models for precipitation have proven in the literature to be powerful tools capable of describing complex precipitation processes, whether isothermal or non-isothermal, including several types of precipitates, non-stoichiometric phases, etc.

We have shown in this article that modelling of the so-called reversion experiments allows us to obtain independently information on three parameters of the precipitating system: the diffusion constant, solubility at the reversion temperature, and interfacial energy. Most importantly, these parameters are obtained without any interference with precipitate nucleation, which generally requires a separate, independent modelling effort.

Of course, this model-based calibration of physical parameters requires high quality data so as to obtain the evolution of average size and volume fraction, preferably in situ. To our knowledge such measurements are relatively straightforward in systems where the precipitate composition is well known, using Small-Angle Scattering (SAS) [24].

References

[1] O.H. Bratland, O. Grong, H.R. Shercliff, O.R. Myhr, S. Tjotta, Modeling of precipitation reactions in industrial processing, Acta Mater. 45 (1) (1997) 1–22.
[2] J. Lendvai, Precipitation and strengthening in aluminum alloys, Mater. Sci. Forum 217 (1996) 43–56.
[3] H. Zurob, C. Hutchinson, Y. Bréchet, G. Purdy, Acta Mater. 50 (3075) (2002).
[4] T. Gladman, The Physical Metallurgy of Microalloyed Steels, The Institute of Materials, London, 2002.

[5] M. Hillert, Inhibition of grain-growth by 2nd-phase particles, Acta Metall. 36 (12) (Dec. 1988) 3177–3181.
[6] E. Clouet, L. Laé, T. Epicier, W. Lefebvre, M. Nastar, A. Deschamps, Complex precipitation pathways in multi-component alloys, Nature Mater. 5 (2006) 482–488.
[7] E. Clouet, M. Nastar, A. Barbu, C. Sigli, G. Martin, Precipitation in Al–Zr–Sc alloys: A comparison between kinetic Monte Carlo, cluster dynamics and classical nucleation theory, in: J.M. Howe, D.E. Laughlin, J.K. Lee, D.J. Srolovitz, U. Dahmen (Eds.), Solid–Solid Phase Transformations in Inorganic Materials, TMS, Warrendale, USA, ISBN 978-0-87339-608-0, 2005.
[8] R. Wagner, R. Kampmann, Homogeneous second phase precipitation, in: Materials Science and Technology: A Comprehensive Treatment, vol. 5, John Wiley & Sons Inc, 1991, pp. 213–302.
[9] R. Kampmann, T. Ebel, M. Haese, R. Wagner, A combined cluster-dynamic and deterministic description of decomposition kinetics in binary alloys with a tendency for clustering, Phys. Status Solidi B 172 (1) (1992) 295–308.
[10] O.R. Myhr, O. Grong, Modelling of non-isothermal transformations in alloys containing a particle distribution, Acta Mater. 48 (2000) 1605–1615.
[11] J.D. Robson, Modelling the overlap of nucleation, growth and coarsening during precipitation, Acta Mater. 52 (2004) 4669–4676.
[12] M. Nicolas, A. Deschamps, Characterisation and modelling of precipitate evolution in an Al–Zn–Mg alloy during non-isothermal heat treatments, Acta Mater. (2003) 6077–6094.
[13] M. Perez, M. Dumont, D. Acevedo, Implementation of the classical nucleation theory for precipitation, Acta Mater. 56 (2008) 2119–2132.
[14] P. Maugis, M. Gouné, Kinetics of vanadium carbonitride precipitation in steel: A computer model, Acta Mater. 53 (2005) 3359–3367.
[15] S. Esmaeili, D.J. Lloyd, W.J. Poole, A yield strength model for the Al–Mg–Si–Cu alloy AA6111, Acta Mater. 51 (2003) 2243–2257.
[16] M. Perez, C. Sidoroff, A. Vincent, C. Esnouf, Microstructure evolution of martensitic 100Cr6 bearing steel during tempering, Acta Mater. 57 (2009) 3170–3181.
[17] C. Zener, Theory of growth of spherical precipitates from solid solution, J. Appl. Phys. 20 (1949) 950–953.
[18] J.W. Gibbs, On the equilibrium of heterogeneous substances (1876), in: Collected Works, Green and Co., 1928.
[19] J. Thomson, Theoretical considerations on the effect of pressure in lowering the freezing point of water, Trans. Roy. Soc. Edinburgh 16 (1849) 575–580.
[20] J. Thomson, On crystallization and liquefaction, as influenced by stresses tending to changes of form of crystals, Proc. Roy. Soc. 11 (1862) 473–481.
[21] W. Thomson, On the equilibrium of vapour at a curved surface of liquid, Philos. Mag. 42 (1871) 448–452.
[22] M. Perez, Gibbs–Thomson effect in phase transformations, Scripta Mater. 52 (2005) 709–712.
[23] M. Perez, F. Perrard, V. Massardier, X. Kleber, A. Deschamps, H. De Monestrol, P. Pareige, G. Covarel, Low temperature solubility of copper in iron: Experimental study using ThermoElectric Power, small angle X-ray scattering and tomographic atom probe, Philos. Mag. 85 (20) (2005) 2197–2210.
[24] A. Deschamps, C. Genevois, M. Nicolas, F. Perrard, F. Bley, Study of precipitation kinetics: Towards non-isothermal and coupled phenomena, in: J.D. Embury Honnorary Symposium, Hamilton, Canada, 2005, Philos. Mag. 85 (2005) 3091–3112.